



The Space Congress® Proceedings

1968 (5th) The Challenge of the 1970's

Apr 1st, 8:00 AM

Structural Considerations for Larger Upper Stage Development

Clifford Y. Kam

Missile and Space Systems Division, Douglas Aircraft Company, Santa Monica, California

Karl M. Anderson

Missile and Space Systems Division, Douglas Aircraft Company, Santa Monica, California

Gerald V. Anderson

Missile and Space Systems Division, Douglas Aircraft Company, Santa Monica, California

Follow this and additional works at: <https://commons.erau.edu/space-congress-proceedings>

Scholarly Commons Citation

Kam, Clifford Y.; Anderson, Karl M.; and Anderson, Gerald V., "Structural Considerations for Larger Upper Stage Development" (1968). *The Space Congress® Proceedings*. 4.

<https://commons.erau.edu/space-congress-proceedings/proceedings-1968-5th/session-13/4>

This Event is brought to you for free and open access by the Conferences at Scholarly Commons. It has been accepted for inclusion in The Space Congress® Proceedings by an authorized administrator of Scholarly Commons. For more information, please contact commons@erau.edu.

EMBRY-RIDDLE
Aeronautical University™
SCHOLARLY COMMONS

Clifford Y. Kam, * Karl M. Anderson, ** and Gerald V. Anderson ***
 Missile and Space Systems Division
 Douglas Aircraft Company, Santa Monica, California

1. Introduction and Summary

The selection of design configurations and materials for large vehicles such as those proposed for manned missions to Mars in the early 1980's will require the resolving of major technological questions during the next few years. The structure required to contain the large volume of liquid propellants, particularly hydrogen, must be of efficient design so that payload capability can be maximized. In a typical study recently conducted, design criteria were established for a multimodule upper stage. Each stage module consists of a basic shell structure, an insulated, internally mounted LH₂ propellant tank, and the thrust engine with its associated support system and hardware. Meteoroid protection is incorporated in the shell structure. The largest potential for structural weight-saving appears to be in the LH₂ propellant tank design. Aluminum alloys are currently favored as tank material because of successful experience and the high level of technological development. Titanium alloys, however, offer sizeable potential weight savings because of their superior biaxial strength properties at cryogenic temperatures. The biaxial strengths of titanium alloys range from 30% to 70% greater than their uniaxial strength, compared to less than 15% for the aluminum alloys. However, there are certain requisite programs that must be conducted before titanium can be introduced as a qualified structural material for large cryogenic tankage. This study investigated the following areas: texture strengthening of titanium alloys, nondestructive inspection techniques, critical crack size, proof load levels, compatibility with LH₂ under long-term storage conditions, stress corrosion, creep, and low-cycle fatigue. Only with positive results in these areas could the materials be used. Efficient means of attachment of structural components to thin-gage tanks were studied, as were manufacturing considerations for the vehicles. These included material size, development of welding methods and equipment, and techniques for handling the large, thin-gage upper stage structural components before, during, and after fabrication.

Other areas where improvements could be made are: low conductivity support structure; high-performance insulation with quick evacuations; and truss grid, core sandwich construction for outer shells.

* Chief, Structures Development Branch,
 Member AIAA, ASTM

** Senior Engineer/Scientist, Structures
 Development Branch, Member, AIAA

*** Materials Research and Development
 Specialist, Metals and Ceramics Branch

2. Considerations for Large Upper Stage

2.1 Missions and Schedule

The manned Mars capture and landing mission is one of the NASA objectives proposed in the post-Apollo era. Several studies have been made for manned planetary capture and landing missions to determine vehicle system weights in earth orbit, and technological program requirements. The studies indicate that nuclear rocket propulsion offers an opportunity for efficient manned planetary exploration with vehicles that use nuclear propulsion. The vehicle weights vary from approximately 4.5 million lb in Earth orbit to approximately 1.8 million lb, depending on the mission year. Although this paper discusses a nuclear-stage vehicle, structural considerations presented herein would generally apply to a similar chemically-powered stage.

2.2 Configuration

The three-stage Mars capture and landing vehicle investigated in the design study is composed of five modules: three for the Earth-departure stage, and one each for the arrive-Mars and leave-Mars maneuvers (Figure 1). The module design (Figure 2) is also used in different combinations for multimission capability; i.e., planetary flyby, Venus capture, and Lunar applications.¹

The largest potential for structural weight savings appears to be in the LH₂ propellant tank design. A typical configuration for a propellant tank with approximately 250,000 lb LH₂ capacity would be a welded structure consisting of a straight cylindrical section approximately 54 ft long and 32 ft in diam, with hemispherical domes. The wall thickness of the tank would vary from approximately 0.030 to 0.050 in. for titanium and 0.063 to 0.130 in. for aluminum. Aluminum alloys are currently favored as tank material because of successful experience and the high level of technological development. Titanium alloys, however, offer sizeable potential weight savings because of their superior biaxial strength properties at cryogenic temperatures. The biaxial strengths of titanium alloys range from 30% to 70% greater than their uniaxial strength, compared to less than 15% for the aluminum alloys.

3. Propellant Tanks

There is a wide choice of proven configurations as well as several materials available for the design of propellant tanks. The structure designer must select that configuration and material which contributes to the highest overall structural efficiency of the vehicle.

Studies have been made which compared the structural efficiency of cryogenic tanks fabricated from stainless steel, aluminum, titanium, and fiber-

glass.² The data (Figure 3) for 10- and 30-ft-diam tanks indicate that titanium and fiberglass show the best potential for future cryogenic tanks.

In the nuclear-stage study previously mentioned, a weight comparison was made using aluminum and titanium alloys as affected by design stress levels. Figure 4 shows the results of this comparison. The stress levels shown are for a specific critical design temperature--in this case -160°F, a typical ullage gas temperature condition. The uniaxial to maximum biaxial ultimate tensile strengths (typical, not necessarily design) for several selected aluminum and titanium alloys are also shown in the figure. (The weight scale shown is for the pressure shell only; no allowance is made for local reinforcements for access doors, support structure attachment, cylinder-to-dome joints, etc.) The figure shows that considerable weight saving is possible using a titanium alloy such as Ti-6Al-4V in place of aluminum alloys such as 2014 or 2219.

Tank geometry is also important. The most efficient pressure vessel design is, of course, a sphere. The vehicle design configuration in many cases will not permit a single sphere to be installed because of the large size required to meet volume requirements. When this occurs, multiple spheres or other configuration(s) must be used.

A geometry and weight comparison of various configurations for storing 250,000 lb of LH₂ with an added 5% ullage volume is shown in Figure 5. Two materials, 2014-T6 aluminum alloy and 6Al-4V titanium, were compared. An ullage temperature, -160°F, was used for selection of the material allowables. The weights shown are for the basic pressure-vessel shell with uniform internal pressure, and with no allowance for doors, attach points, joints, etc.

The indicated shell weight ratios in Figure 5 are for a weight comparison of the outer shell as it is affected by the tank geometry, using the cylinder configuration as the basis for comparison with an assigned equivalent value of 100. Only the extra material required due to geometry is included; no provision is made for change of bending moment redistribution of tank support loads, aerodynamic loads, etc. on the vehicle due to the change of length.

3.1 Textured Titanium

With sheet titanium, the designer has the option of using either textured or untextured strength properties.

Texturing refers to a very specific type of anisotropy or preferred orientation developed primarily in metals that have a hexagonal close-packed crystal structure. When these metals (of which titanium is one) are loaded biaxially in tension, the orientation of the crystal structure tends to limit the ability of the metal to deform in the thickness direction, thus increasing the strength in the plane of the sheet. Various methods have been investigated for determining the degree of texturing in hexagonal close-packed metal systems. The methods are discussed in the following paragraphs.

Uniaxial Tension - This method utilizes a stacked biaxial strain gage in the center of the reduced section of a uniaxial tensile specimen.

The degree of texturing is related to a value R, which can be expressed by the equation:

$$R = \mu_p / (1 - \mu_p) \quad (1)$$

where

μ_p = Poisson's ratio in the plastic region of the stress-strain curve.

The value of μ_p can be determined by measuring the linear slope of the plot of longitudinal strain (ϵ_L) versus transverse strain (ϵ_T) in the plastic region, as obtained from the biaxial strain gage. Values of R greater than 1.0 indicate texture strengthening ($\mu_p > 0.5$). Tests conducted by Douglas on textured titanium alloys have compared the results of uniaxial tensile tests (with biaxial strain gages) to the results of biaxial burst tests (pressure vessels) in the same heat of material. The uniaxial tensile R value data predicts the biaxial yield locus correctly, but not the burst.³

A major weakness in this procedure is that as the width-to-thickness ratio of the uniaxial specimen is increased (thin specimens), the stress state in the center of the specimen changes from uniaxial to biaxial because of restraint effects. This restraint affects the width strain, which in turn affects R.

Uniaxial Thickness Compression - This test method essentially consists of two platens which compress a stack of washers from the sheet material being investigated. Enough washers are prepared to make a stack approximately 3 in. high. Strain gages 90° or 120° apart are bonded in the center of the stack. The washers are placed over an alignment pin and encapsulated in a plastic resin. The specimen is then tested in a compression testing machine.

Assuming hydrostatic tension does not produce yielding, uniaxial thickness compression is equivalent to a 1:1 balanced biaxial tension stress state.

This is illustrated in Figure 6. The following equation relates R to the compressive yield stress in the thickness direction and the uniaxial tensile yield strength in the plane of the sheet, assuming planar anisotropy.³

$$R = (2S_3 - S_1) / S_1 \quad (2)$$

where

S_3 = compressive yield strength.

S_1 = tensile yield strength.

While this equation is usually associated with the 0.2% yield stress, it is valid for any strain on the stress-strain curve in the plastic region as well. Note that if work hardening occurs in the compression thickness test (S_3), but not in the conventional tension test (S_1), R must increase with increasing plastic strain. The above behavior would predict

that work hardening would occur in a 1:1 biaxial test also (spherical pressure vessel). Such behavior has been noted for titanium sheet. ⁴

Figure 7 is a typical plot of various R values to demonstrate the practical meaning of R in terms of texture strengthening in biaxial fields.

Pressure Vessels - The most accurate method for determining the degree of texturing in titanium alloys is to fabricate and test pressure vessels of the material in question. However, this is probably the most expensive method.

The configuration used by Douglas consists of a cylindrical specimen anchored into two end-fittings which permit both axial load and internal pressure to be applied to the specimen simultaneously. The specimens are roll-formed from sheet material into 4-in. -diam cylinders, GTA-welded along the longitudinal seams, and then chemically milled in the areas to be tested. The cylinder ends are trimmed and manually GTA-burned-down to provide a bead on the edges of the cylinder ends. The cylinders are fastened to reusable end-fittings by means of a wedge-shaped joint filled with Cerrobend. Using this setup, specimens can be tested at room temperature and cryogenic temperatures in 1:2, 1:1, and 2:1 biaxial stress fields. ⁵

Studies conducted by Douglas indicate (with the exception of actual pressure vessel specimens) that the uniaxial thickness compression test is the most reliable method for determining the degree of texturing of titanium alloy sheet. It is able to predict not only the correct yield locus R value for a 1:1 biaxial tension test (pressure vessel), but the work hardening that occurs during such a biaxial test as well.

3.2 Weld Properties

Uniaxial tensile tests have been performed on parent and welded Ti-5Al-2.5Sn ELI and Ti-6Al-4V ELI at room temperature and -423°F. Biaxial tests were conducted by Douglas at -423°F on parent and welded Ti-6Al-4V ELI. The biaxial tests were made using 4-in. -diam cylinders, gas tungsten arc (GTA) welded without filler wire. The test areas, parent and welded, were chemically milled to 0.06 in. from 0.020 in. Figure 8 shows biaxial burst data for Ti-5Al-2.5Sn ELI and Ti-6Al-4V ELI. Based on these tests, a reasonable assumption would be that the welds (GTA) exhibit the same strength as the parent metal. Plain strain fracture toughness data at -423°F for GTA and electron beam welds, however, indicate a fracture toughness approximately 25% and 17% lower, respectively, than that of the parent metal.

3.3 Additional Tank Material Consideration

Further analysis points up several areas for consideration. In order to proof-test a titanium pressure vessel for a safe-life design, it is necessary to select the proof pressure based on the fracture toughness of the weld rather than the parent material. It also indicates that the use of built-up weld lands to reduce the stress in the welds, may, in some instances, mask the significance of a proof test.

3.3.1 Long-Term Storage Compatibility. Sustained load tests were conducted by Douglas at room temperature on precracked specimens of annealed Ti-6Al-4V ELI parent material. Loads below 80% of yield were insufficient to cause failure in a reasonable time period. The specimens were tested in a gaseous hydrogen (GH₂) atmosphere. The results indicate that sustained load failures in GH₂ at room temperature can be a problem if a fresh crack is present (i. e., the crack is extended in GH₂), and the local stress intensity is quite high. If the crack is not extended in GH₂, no attack appears to be evident.

To determine temperature dependence, fatigue tests were also conducted on precracked specimens at temperatures ranging from room temperature to -423°F. These tests were conducted in GH₂, LH₂, and inert atmospheres (N₂ or He). The test results indicate that below -100°F there is no effect on material properties by either GH₂ or LH₂. At temperatures above -100°F in a GH₂ environment, the crack propagation rate slowly increases until at room temperature it is greater by a factor of approximately 2. The criteria for attack on titanium by GH₂ appear to be a moderately high temperature (above -100°F) and a fresh surface with no oxidizing elements present. It has been found that a slight oxygen contamination in the gaseous environment will prevent attack.

4. Tank Support Structure

The primary function of a propellant tank-support system is to accomplish what the name implies: support the tank within the outer load-carrying shell. The support configuration (size, thickness, and required strength) is a function of the boost profile and the propulsion module weight. Unfortunately, the support becomes a direct heat short between the shell and the tank and may cause considerable boiloff of cryogenic fuels such as LH₂. Because of this, the support structure design becomes a tradeoff between the structural load and stability requirements, and the heat conducted to the fuel tank.

Cryogenic tank support systems can be categorized in two basic design concepts: (1) continuous supports that completely gird the fuel tank, and (2) point supports that contact the tank at a minimum number of locations. Continuous support is desirable because all of the thrust loads are distributed uniformly (rather than concentrated), and a minimum amount of internal tank and shell reinforcing is required. However, this configuration may present greater contact area, cause greater heat flux and fuel boiloff, and create a larger thermal contraction problem. On the other hand, a point support system requires the least cross-sectional area and lessens the heat flux through the support. Because of highly concentrated loads, however, the point support system requires more internal tank structure and support shell structure.

The structure must be designed to minimize load concentration created by thermal shrinkage, and expansion due to pressure. A 32-ft-diam by 85-ft-long thin-gage titanium tank will shrink approximately 0.75 in. in diam and 1.9 in. in length, due to exposure to LH₂ temperature (-423°F); and it will expand up to 2.25 in. and 4.0 in. respectively at 35 psi internal pressure.

These deflections must be considered in the tank support design. If the tank is relatively long, say an L/D ratio of 1.5 or greater, stabilizing members may need to be provided. These must be arranged to minimize loads in the tank shell due to the deflections mentioned above, and to minimize the transfer of body shell loads to the tank. Insulation (see Section 5) must also be considered, particularly in tank-to-support attachment areas.

Several interesting concepts have been proposed for tank support structure. Figure 9 shows a continuous cone with several variations, such as with and without stiffeners and lightning holes, and provisions for cooling coils using the vent gases from the tank. While a tension cone is shown, the figure also applies for a compression cone. Another variation is the cone-shaped truss arrangement shown in Figure 10. A point attachment support system using collimated fiberglass-tape tension rods is shown in Figure 11. A variation of the point attachment is the concept which uses a device for retracting the main structural attachments to the tank after boost to orbit.

Thermal effectiveness of the tank support structure must be regarded as a part of the effectiveness of the entire propellant system of the stage. The propellant boiloff effective weight must be added to the weight of the structure to obtain a basis for design trades.

In a preliminary design study, a continuous compression cone structure was investigated. The cone geometry was as follows: diam 105-in., straight-tapered to 120 in., by 24 in. high. The LH₂ tank was attached to the small end, imparting a design load of 1, 173 lb/in., including a 1.4 margin-of-safety factor. In this study, a corrugated fiberglass configuration was found to be the lightest structurally, but a tubular strut support configuration (similar to that shown in Figure 10) was found to have the lowest propellant boiloff and total weight, as shown in Figure 12. Further studies would be required to optimize the system for nuclear stage sizes.

5. Insulation Considerations

For long-term space missions such as those proposed for the nuclear stage, the thermal protection system becomes a dominant consideration. Analyses and experiments have proved that high-performance insulation (HPI) systems are quite capable of providing that thermal protection.

HPI has been chosen because it is about three orders of magnitude more effective than typical foam insulation. However, if the full potential of HPI is to be obtained, the following considerations must be met:

1. Accurate thermal prediction.
2. Insulation application in a manner to insure insulation survival under boost loads (evacuation, inertia, sonic, and vibration).
3. Insulation application insuring evacuation of purge gases to a pressure of 10^{-4} torr soon after boost.
4. Isolation of heat through vehicle structure and plumbing.

5. Definition of an optimum basic insulation system.

The results of insulation tests at Douglas comparing three types of multilayer insulation systems is shown in Figure 13. The insulation was mounted on a spherical liquid hydrogen tank containing 950 lb of propellant. Helium, nitrogen-purged, and evacuated-bag systems were considered. The data indicates that helium-purged systems are the most attractive for longer mission durations. In a purged system, the time to evacuate the purge gas after launch is typically 2 to 12 hr. Perforations in the insulation can speed up evacuation and still result in low thermal penalties, provided the perforated area is less than 2% of the total area.

Figure 14 shows the sources of heat entering a typical propellant system for a 14-day mission. Heat enters a tank through the insulation, including the basic insulation; conduction through the purge gas; joints and attachments; tank supports; and plumbing. Overlapping joints and seams can be constructed with a thermal penalty between 0 and 0.05 btu/hr/in ft. HPI blankets can be attached with a discontinuous fastener to prevent the shorting out of each sheet. Heat transfer through tank supports can be minimized with insulated, high-strength fiberglass rods. Pipeline heat flux can be reduced by an order of magnitude with nonmetallic isolation units. Heat transfer resulting from insulation penetration by supports, and cutouts for supports, can be practically eliminated by stringent design.

6. Outer Shell and Engine Support Structure

To ensure reliability and minimum weight, outer shell design must take into consideration (1) load-carrying structure, (2) insulation protection, and (3) meteoroid protection.

The most severe design condition for the outer shell usually occurs at maximum α . In many cases, a margin-of-safety factor of 1.25 is applied to the limit loads to obtain their ultimate value for unmanned flight, and a factor of 1.4 is used for manned flight. In the final design, these factors should be reviewed; numbers should be established based on the fracture mechanics of the material, and expected load environments and intensities, including the lifetime cycling load histories.

The relative weights of optimum-proportioned structures suitable for use in the vehicle structure are shown in Figure 15.^{6, 7, 8} It should be emphasized that actual structural weights would be greater than those shown in the figure which shows theoretical optimums only. For instance, there is no allowance for joints, access doors and cutouts, end closure frames, stringer eccentricities, and concentrated load points.

While the figure shows a decided weight-saving potential for the newer materials as compared to aluminum (particularly in the lower load intensities) remember that manufacturing and processing technologies required for their use in a large upper stage are not nearly as fully developed as are those for aluminum.

As mentioned previously, the most severe design condition for the outer shell occurs during boost to Earth orbit. Once the stage is ready to be

fired for its part of the mission, the shell requirements are reduced substantially. HPI protection of the tank from meteoroids appears to be adequate during the short engine burn-time. Therefore, jettisoning the outer shell, or as much of it as possible, just prior to starting the engines, appears to be an attractive means of improving structural efficiency.

The jettisoning operation would use a separation system similar to the one being used in payload firings of Agena and other systems. It provides a contamination-free separation with no outgassing and no fragmentation; it has been developed to the state where final velocity imparted to the shroud segments can be accurately predicted. The reliability of the joint has been successfully demonstrated in numerous tests and flights of full-size hardware.

The engine support structure would probably be very similar to the outer shell configuration, since it will be designed primarily for the compression loads generated during engine burning. Particular attention must be paid to isolating the engine thermally as much as possible from the cryogenic fuel tank in order to have minimum propellant boiloff. This applies to the engine feed lines as well as the support structure. Conical structures of nonmetallic fiberglass sandwich or corrugations appear to be the most efficient configurations.

7. Meteoroid Protection

Extended space missions impose a severe meteoroid environment on the spacecraft and propulsion stages. Protection against meteoroids can add a substantial weight penalty. This is particularly critical for a large stage such as the nuclear stage, because of the large volume of vulnerable tankage required for liquid hydrogen propellant. The stage size, and the ambitious nature of most missions such as manned extended-orbit and interplanetary exploration, provide a substantial premium for development of an efficient stage configuration with combined thermal insulation and meteoroid protection functions.

The uncertainty of the meteoroid environment during the Mars mission creates some problems in determining the design criteria for meteoroid protection. Factors to be considered in the design include meteoroid flux, mass, density, velocity, angle of impact, etc. Considering the uncertainties in the design environment and the limited validity of analytical methods, one approach would be to define the threshold of perforation, or ballistic limit of the structure, as a function of plate spacing and projectile.

Recent studies at the Douglas Ballistic Range indicated that the truss-grid honeycomb sandwich construction shown in Figure 16 will provide adequate meteoroid protection consistent with efficient structural performance. Further analyses for nuclear stages may require additional foam protection between the outer shell and the tank insulation, depending on meteoroid flux and velocity models. The selected HPI mounted on the tank, is effective for stopping debris produced when the meteoroid is broken up by the outer shell.

A series of tests with sapphire projectiles has been conducted at the Douglas Aerophysics Laboratory Ballistic Range. Sapphire was selected as representative of a typical asteroidal meteoroid likely to be encountered during long-duration missions.

Range velocities of 24,000 to 28,000 ft/sec used in the tests are closer to the average velocities expected at 1.5 to 2.0 AU than at 1.0 AU. Hence, the data are considered to be a fairly good representation of impact effects to be encountered in the 1.5 to 2.0 AU region.

Figures 17, 18, and 19 show typical results obtained in current tests. Note that, aside from some small craters, no significant damage was done to any of the structural wall "witness plates". It is of particular interest to note that removing the 2-in. truss grid core produced a somewhat larger spray area, but there was no significantly greater structural damage in terms of wall penetration. This is because of the effectiveness of the two 20-mil face sheets plus 100 layers of insulation in fragmenting the projectile and bumper debris. The velocity of the projectile was reduced from 26,700 ft/sec to 24,300 ft/sec in order to establish the ballistic limit with no honeycomb core between the outer face sheets.

Since the first sheet target ($t_s = 0.020$ in.) remains close to optimum, the 100-plus layers of multisheet insulation are very effective in fragmenting and stopping high-velocity projectile/bumper fragments.

A comprehensive evaluation of meteoroid impact effects is considered essential to design efforts on stages for long-term storage of liquid propellants in space. When defining design criteria for the vehicle, the tolerable amount of tank wall damage should be specified; for example, the limit of crater marks (or none whatever) resulting from specified mass and velocity of projectiles representative of the expected meteoroid environment. Tests should be conducted on configurations of finite sheet-truss grid core combinations involving aluminum, beryllium, and titanium as structural materials. In addition, several high-performance insulation concepts should be tested for resistance to meteoroid debris penetration.

From a meteoroid protection standpoint, beryllium and aluminum are considered to be equal in these types of configurations. Therefore, in cases where meteoroid protection predominates over launch loads for sizing the skins, the use of aluminum is dictated because of the cost factor.

8. Manufacturing Considerations

Development of current hardware has required extension of manufacturing techniques and processes on a large scale compared to those required for the predecessor programs. Many of these are applicable to nuclear upper stages, but there are problem areas that need further development, especially in the area of large thin-gage tank fabrication and insulation. The large outer shell structure will also pose some problems.

The two major candidate materials for the tank structure are titanium and aluminum alloys. While these have been successfully and routinely welded

in industry, certain techniques and problem areas will require further development--especially for titanium, which appears to be the most attractive tank material from the standpoint of structural efficiency.

8.1 Material Size and Availability

The maximum titanium sheet width presently available in the 0.050-in. thickness range is 4 ft. This somewhat limited width, even in the next decade, will mean that a substantial amount of weld footage will be required for fabrication of large titanium tanks.

8.2 Handling of Large Thin-Gage Sheets

The thin-gage materials proposed for the nuclear stage will require careful handling during all stages of the manufacturing operation to prevent the occurrence of dings, creases, and tears in the sheets.

8.3 Tank Fabrication

A possible fabrication and assembly procedure for the hemispherical domes of the nuclear stage tank has been studied. Figure 20 is a pictorial flow chart showing the operations.

A fabrication and assembly sequence for the cylindrical portion of the large tank is shown in Figure 21. The dome concept would be used, except that the contoured pallets would not be required.

Final assembly can be accomplished by rotating the tank in the horizontal or vertical position. Both methods are currently used by major aerospace companies in the fabrication of the Saturn stages.

8.4 Final Assembly of Vehicle

After the tank is finished, it must be leak-checked and cleaned before the multilayered insulation is applied to the exterior surface. Final installation in the vehicle can be accomplished either by building up the outer shell as rings around the tank, or

by inserting the insulated tank into the previously completed shell assembly. In either case, provision must be made to prevent damage to the fragile insulation and the thin-walled tank shell during final assembly.

REFERENCES

1. R. J. Holl. Nuclear Design Study. Douglas Aircraft Company Report No. DAC 57976, January 1967.
2. H. H. Dixon. Structural Research and Development for Cryogenic Stages. Douglas Aircraft Company Engineering Paper No. 3963, 24 September 1966.
3. D. L. Corn. A Comparison of the Uniaxial Compression Thickness and Planer Tension Methods for Predicting the Biaxial Properties of Alloyed Titanium. Douglas Aircraft Company Report No. DAC 59533, 6 January 1967.
4. H. W. Babel and D. L. Corn. A Comparison of Methods for Correlating Texturing with the Biaxial Strengths of Titanium Alloys. Douglas Aircraft Company Paper No. 3738, 9 March 1966.
5. H. W. Babel, D. A. Eitman and R. W. McIver. The Biaxial Strengthening of Textured Titanium. Douglas Aircraft Company Paper No. 3471, June 1965.
6. G. E. Wightman. Beryllium and Light Alloys Technology Development. Douglas Aircraft Company Unpublished Report.
7. F. R. Shanley. Weight-Strength Analysis of Aircraft Structures, (McGraw-Hill Book Company, Inc., New York, 1952) 1st Ed.
8. R. F. Crawford and A. B. Burns. Minimum Weight Potentials for Stiffened Plates and Shells. Jr. Spacecraft Rockets, January 1963, pp. 879-886.

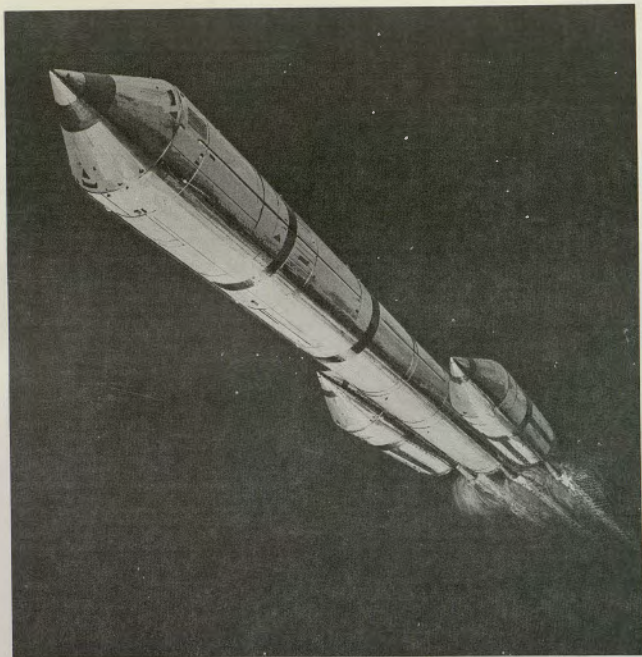


FIGURE 1. NUCLEAR VEHICLE "LEAVE EARTH ORBIT" CONFIGURATION

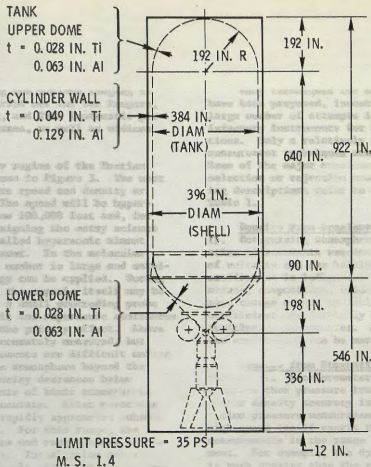


FIGURE 2. LARGE NUCLEAR STAGE

WEIGHT INCLUDES BASIC SHELL,
 ACCESS DOORS AND SUPPORTS

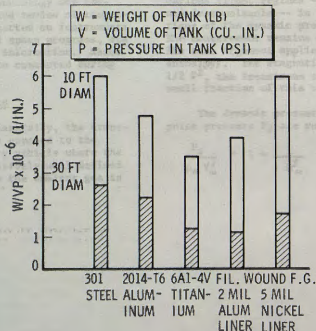


FIGURE 3. STRUCTURAL EFFICIENCY OF CRYOGENIC TANKS

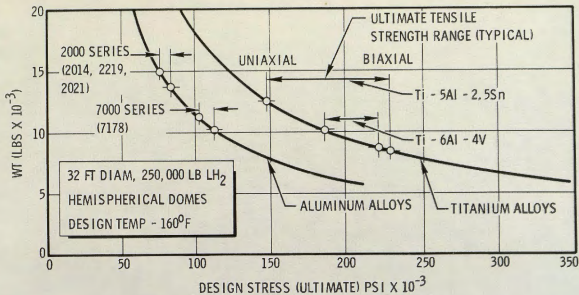
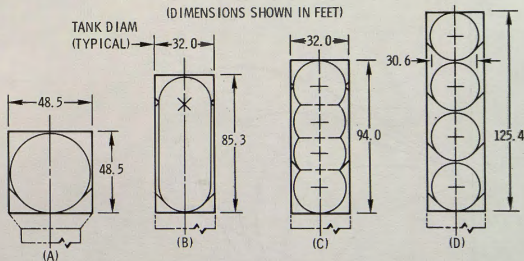


FIGURE 4. TANK WEIGHT COMPARISON, PRESSURE SHELL ONLY



	(A) SINGLE SPHERE	(B) CYLINDER	(C) SEGMENTED SPHERES	(D) MULTIPLE SPHERES
TANK WEIGHTS				
2014-T6 ALUMINUM	11,000	13,600	12,100	12,100 LB
6AL-4V TITANIUM	5,650	6,950	6,200	5,650
SHELL WEIGHT RATIO	85.4	100	110	147

VOL = 60,069 FT³, DES. PRESSURE = 50.0 PSI, DES. TEMP = 160°F

FIGURE 5. TANK CONFIGURATION COMPARISON

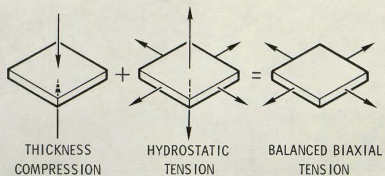


FIGURE 6. UNIAXIAL THICKNESS COMPRESSION EQUIVALENCY

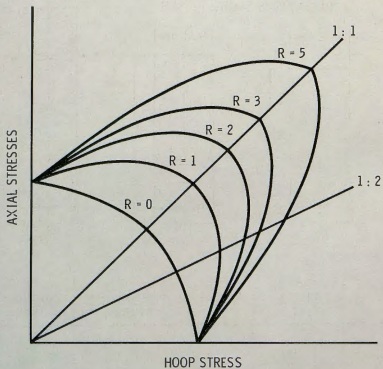


FIGURE 7. YIELD SURFACES FOR VARIOUS R VALUES

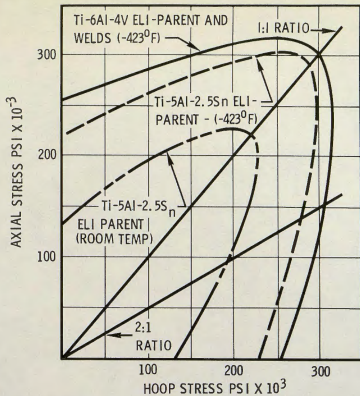


FIGURE 8. BIAXIAL BURST DATA, ROOM TEMPERATURE AND -423°F

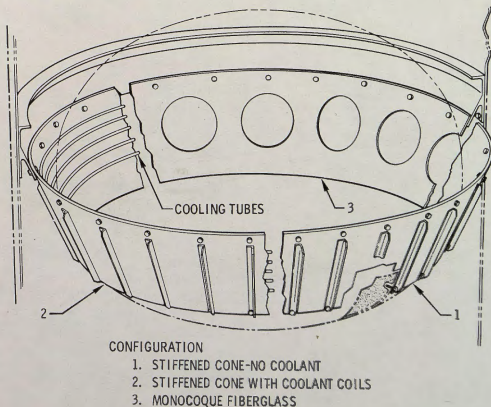


FIGURE 9. CONTINUOUS TENSION CONE SUPPORT SYSTEM

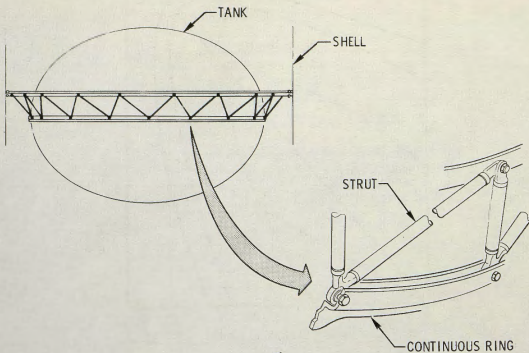


FIGURE 10. CONE-SHAPED TRUSS

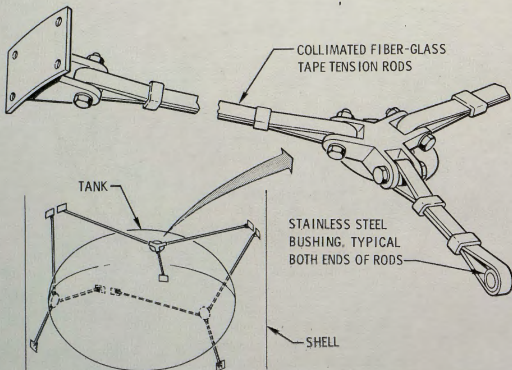


FIGURE 11. MULTIPLE-POINT (3) TENSION ROD SUPPORT SYSTEM

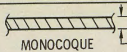
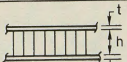
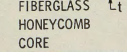
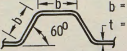
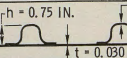
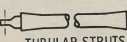
No.	CONFIGURATION	DESCRIPTION	STRUCTURE WEIGHT (LB)	EFFECTIVE BOIL-OFF WEIGHT (LB)	EFFECTIVE TOTAL WEIGHT (LB)
A	 MONOCOQUE $t = 0.25$ IN.	FIBERGLASS LAMINATE	163	492	655
B	 FIBERGLASS LAMINATE FACE SHEETS $t = 0.028$ IN. $h = 0.95$ IN.	FIBERGLASS LAMINATE FACE SHEETS	115	273	388
C	 FIBERGLASS HONEYCOMB CORE $t = 0.015$ IN. $h = 0.60$ IN.	2014 - T6 AL. ALLOY FACE SHEETS	99	24,300	24,400
D	 $b = 1.4$ TO 1.6 IN. $t = 0.062$ IN.	FIBERGLASS LAMINATE CORRUGATION	73	280	353
E	 $h = 0.75$ IN. $t = 0.040$ IN. $t = 0.030$ IN.	FIBERGLASS LAMINATES SKIN AND STRINGER	76	270	346
F	 TUBULAR STRUTS	FIBERGLASS LAMINATE	81	237	318

FIGURE 12. WEIGHT SUMMARY OF TANK SUPPORT CONFIGURATIONS

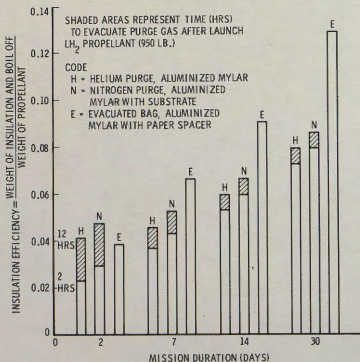


FIGURE 13. COMPARISON OF PURGED AND EVACUATED INSULATION SYSTEMS

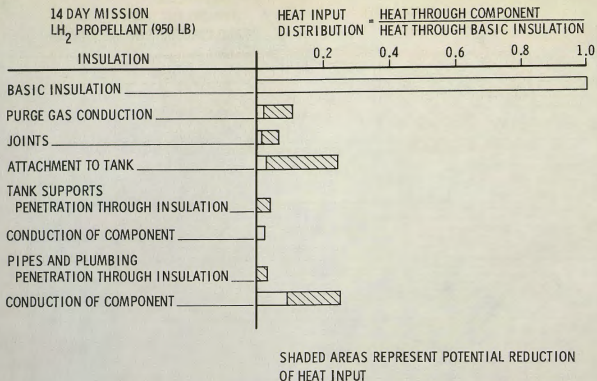


FIGURE 14. HEAT TRANSFER THROUGH VARIOUS COMPONENTS

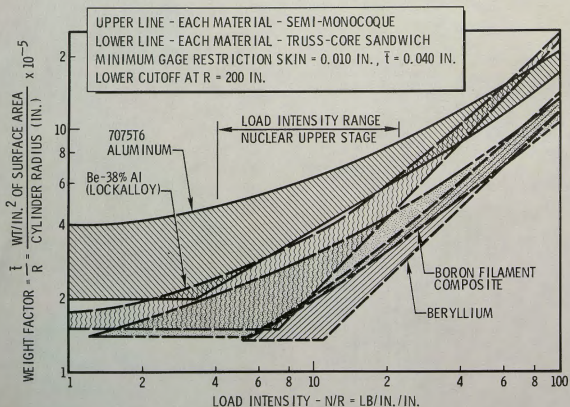
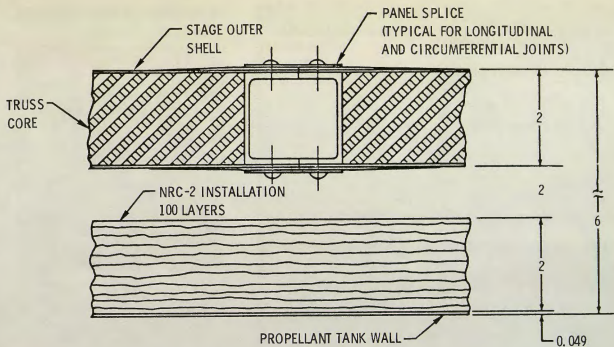
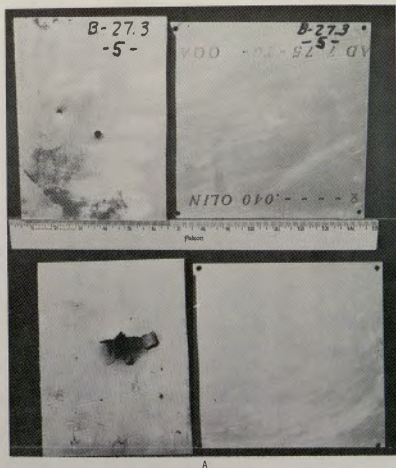


FIGURE 15. OPTIMUM WEIGHTS - CYLINDER AXIAL COMPRESSION



NOTE: ALL DIMENSIONS ARE IN INCHES.

FIGURE 16. CROSS-SECTION THROUGH OUTER SHELL, NRC-2 INSULATION, AND PROPELLANT TANK

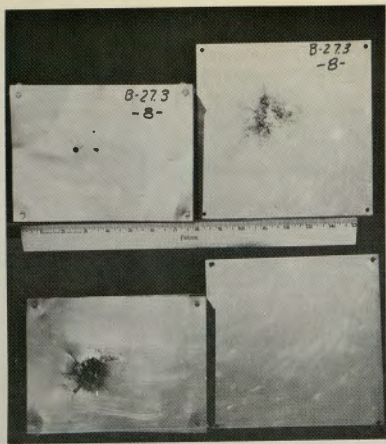


- A. UPPER LEFT - INNER SURFACE, OUTER SHEET
 LOWER LEFT - INNER SURFACE, INNER SHEET
 UPPER RIGHT - OUTER SURFACE, TANK SKIN
 LOWER RIGHT - INNER SURFACE, TANK SKIN

- B. EFFECTS OF PROJECTILE - BUMPER DEBRIS ON 100 LAYERS OF NRC-2 THERMAL INSULATION

0.020 IN. 7075-T6 ALUMINUM ALLOY FACE SHEETS
 2.0 IN. ALUMINUM TRUSS GRID HONEYCOMB CORE
 0.125 DIAM SAPPHIRE PROJECTILE, 0.066 GRAMS
 VELOCITY - 26,700 FT/SEC

FIGURE 17. METEOROID IMPACT TESTS



A



B

- A. UPPER LEFT - INNER SURFACE, OUTER SHEET
 LOWER LEFT - INNER SURFACE, INNER SHEET
 UPPER RIGHT - OUTER SURFACE, TANK SKIN
 LOWER RIGHT - INNER SURFACE, TANK SKIN

- B. EFFECTS OF PROJECTILE - BUMPER DEBRIS
 ON 100-LAYER NRC-2 THERMAL INSULATION

0.020 IN. 7075-T6 ALUMINUM ALLOY FACE SHEETS
 2.0 IN. SEPARATION, NO HONEYCOMB CORE
 0.125 IN. DIAM SAPPHIRE PROJECTILE 0.066 GRAMS
 VELOCITY - 24,300 FT/SEC

FIGURE 18. METEOROID IMPACT TESTS

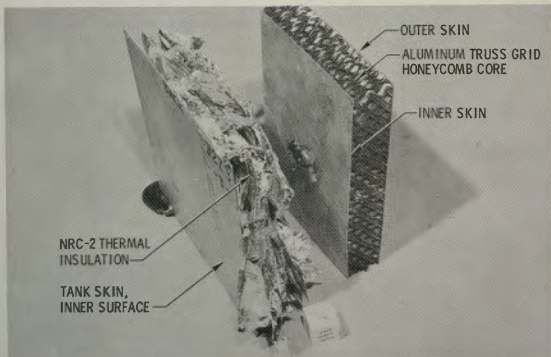


FIGURE 19. THREE-DIMENSIONAL VIEW OF METEOROID IMPACT TEST

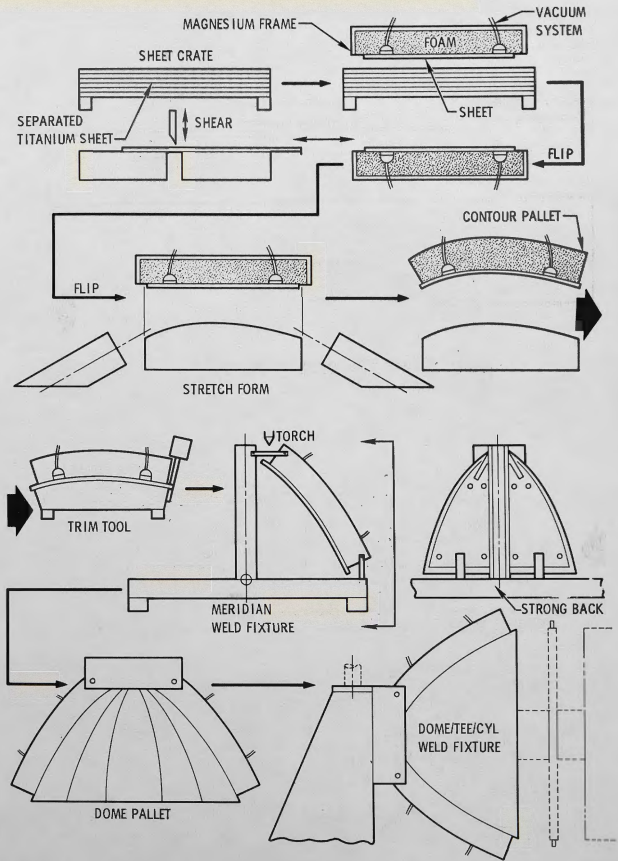


FIGURE 20. FLOW CHART FOR DOME FABRICATION

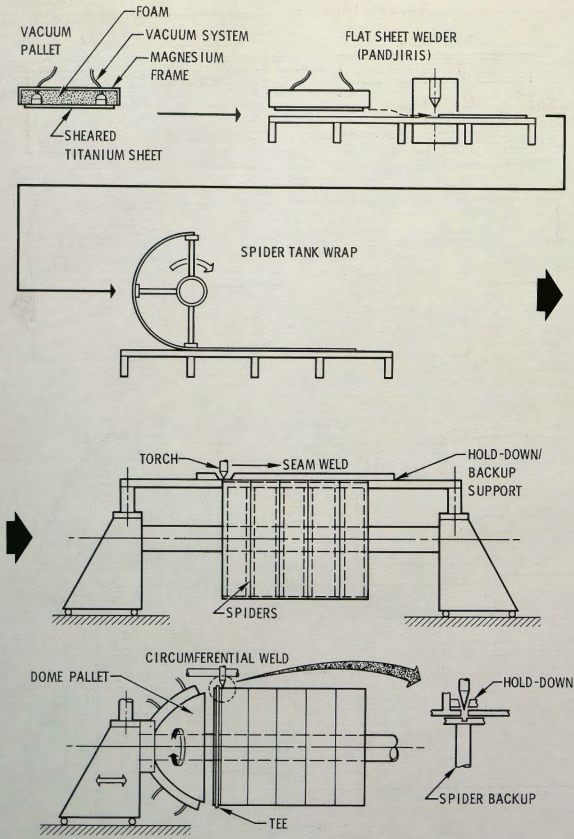


FIGURE 21. FLOW CHART FOR CYLINDRICAL TANK FABRICATION